Cement bonded fine hematite and copper ore particles as oxygen carrier in chemical looping combustion

Xin Tian, Haibo Zhao *, Jinchen Ma

State Key Laboratory of Coal Combustion, School of Energy and Power Engineering, Huazhong University of Science and Technology, Wuhan 430074, PR China

HIGHLIGHTS

- Waste fine hematite and copper ore particles are reused by cement bonding.
- The copper ore to hematite mixing ratio is optimized at 20:80 in weight.
- Integrated merits of hematite and copper ore are achieved in a single particle.
- The $CaAl_2SiO_7$ phase acts as a perfect inert support to inhibit OC sintering.

ARTICLE INFO

ABSTRACT

In this work, bimetallic oxygen carriers (OCs) were prepared from waste fine particles (<0.1 mm) of natural copper ore and hematite for possible application in chemical looping combustion (CLC) processes. The mixtures with different mass ratios of copper ore to hematite were physically bonded by 20 wt% of calcium aluminate cement to obtain OC particles with relatively high disperse structure and good mechanical strength. Cyclic isothermal redox tests were first conducted in a thermogravimetric analyzer (TGA) to optimize the copper ore to hematite mixing ratio in the bimetallic OC. Synergistic effect between copper ore and hematite was observed, and the copper ore to hematite mixing ratio was optimized at 20:80 (namely Cu20Fe80@C) based on a comprehensive consideration of OC reactivity, economic cost and auto-thermal balance in fuel reactor. Subsequently, performance of Cu20Fe80@C and Fe100@C (cement bonded pure hematite) were further evaluated in a batch fluidized bed reactor, using coal as fuel. The Cu20Fe80@C was found to be more reactive towards coal gasification products than that of Fe100@C, which is mainly attributed to the synergistic effect attained by the coexistence of copper ore and hematite in the Cu20Fe80@C OC. Moreover, the effects of steam concentration, oxygen to fuel ratio and coal type on the performance of Cu20Fe80@C were investigated. It was found that both the increase of steam concentration and oxygen to fuel ratio can facilitate the coal conversion, but they are not the higher the better and should be balanced between coal conversion and operational cost when turning to industrial application. Lignite was more suitable to be converted by Cu20Fe80@C OC in *i*G-CLC process due to its better gasification reactivity than anthracite. 30 cyclic redox tests with lignite showed that Cu20Fe80@C exhibited superior redox reactivity, nice fluidization behavior and good anti-sintering property in fluidized bed tests. This work demonstrated that cement bonded fine particles of hematite and copper ore could be a promising and competitive OC candidate for industrial application in *i*G-CLC processes.

© 2017 Elsevier Ltd. All rights reserved.

1. Introduction

Growing concerns on global warming phenomenon, which most probably stems from large quantity of anthropogenic greenhouse gas emission, have resulted in worldwide research efforts to come up with innovative and efficient combustion techniques which can reduce CO_2 emission during fossil fuel combustion processes [1–3]. Among the state-of-the-art carbon capture and sequestration (CCS) technologies [4,5], chemical looping combustion (CLC) has been viewed as one of the most promising approaches due to its inherent CO_2 separation characteristic as well as particularly low energy penalty [6]. For a typical CLC unit, it usually consists of two coupled reactors, *i.e.*, fuel reactor (FR) and air reactor (AR). A kind of solid

---

* Corresponding author.
 E-mail address: hzhao@mail.hust.edu.cn (H. Zhao).

Nomenclature

Cu20Fe80@C	mixed copper ore and hematite (mixing ratio of 20:80 in weight) with 20 wt% of cement
Fe100@C	pure hematite mixed with 20 wt% of cement
F_{N2}	the inlet flow rate of N_2 (mL·s^{-1})
$F_{out, red}$	the instantaneous outlet gas flow rate (dry basis) (mL·s^{-1})
m	the instantaneous weight of the OC (mg)
m_o	the weight of the OC at fully oxidized state (mg)
m_r	the weight of the OC at fully reduced state (mg)
m_0	the weight of the OC at the beginning (mg)
Me	oxygen carrier in reduced state
MeO	oxygen carrier in oxidized state
R_0	the oxygen carrying capacity of the OC (–)
t_0	the time point at the start of the reduction stage (s)
t_{total}	the time point at the end of the reduction stage (s)
x_c	the carbon conversion rate (s^{-1})
x_{inst}	the instantaneous carbon conversion rate (s^{-1})
x_r	the weight loss rate of the OC with synthesis gas (s^{-1})
X_c	carbon conversion (–)
X_r	the weight loss ratio of the OC with synthesis gas (–)
y_i	the instantaneous volume fraction of species i (CO_2, CO, CH_4, H_2 and O_2) in flue gas (–)

Greek symbols

Ω	the oxygen to fuel ratio (–)
γ_i	the gas yield of species i (CO_2, CO, CH_4) (–)

$\gamma_{H2/C}$	the gas yield of H_2 to total carbonaceous gas products (–)

Abbreviations

AR	air reactor
CCS	carbon capture and sequestration
CLC	chemical looping combustion
CLOU	chemical looping with oxygen uncoupling
DTA	differential thermal analysis
ECD	electron capture detector
EDX	energy dispersive X-ray spectroscopy
ESEM	environmental scanning electron microscope
FR	fuel reactor
FS	full scale accuracy
FTIR	Fourier transform infrared spectrometry
GP	Gaoping anthracite from China
iG-CLC	*in-situ* gasification chemical looping combustion
NDIR	nondispersive infrared analysis
OC	oxygen carrier
SL	Shengli lignite from China
TCD	thermal gas conductivity
TGA	thermogravimetric analyzer
XRF	X-ray fluorescence
XRD	X-ray diffraction

metal oxide, known as oxygen carrier (OC), circulates between FR and AR to transfer lattice oxygen needed for fuel conversion. In other words, high metal valence OC (MeO) is reduced by fuel in FR and the reduced OC (Me) regenerates itself by air oxidizing in AR. As FR and AR are structurally interconnected but atmosphere-isolated, the outlet gas of FR mainly consists of CO_2 and H_2O, highly enriched CO_2 stream can be obtained after a simple steam removal process [7].

Due to the large reserve and low price of coal, much more attention has been focused on coal-direct CLC process during recent years [8–12]. Basically, three possible ways have been proposed to realize coal-derived CLC processes, *i.e.*, *ex-situ* gasification chemical looping combustion, *in-situ* gasification chemical looping combustion (*i*G-CLC) and chemical looping with oxygen uncoupling (CLOU) [13]. As additional gasification and air separation units are required, the first way is considered to be economically unfavorable. For the second way, the coal gasification process and gas-solid reaction between OC and gasification products occur in FR simultaneously, so as to avoid the separated gasification unit. While for CLOU, a kind of OC which can release gaseous O_2 in FR is employed, thus direct combustion of coal with O_2 in FR is realized. In this paper, research work will be focused on *i*G-CLC. Fig. 1 depicts the general flow path of *i*G-CLC. As it can be seen that both coal and OC particles are fluidized by gasification agent (CO_2 and/or H_2O) in FR, where complicated heterogeneous and homogeneous chemical reactions, *e.g.*, coal pyrolysis, coal char gasification and OC reduction by gasification products, are taking place. Subsequently, the OC after being reduced in FR is further transported back into AR for regeneration. The possible chemical reactions for typical coal-derived *i*G-CLC process have been summarized in literature [14].

For industrial implementation of chemical looping processes, the selection of suitable OC matters a lot. An appropriate OC should have sufficient oxygen donating capacity, satisfactory reactivity, good resistance to sintering and agglomeration as well as being
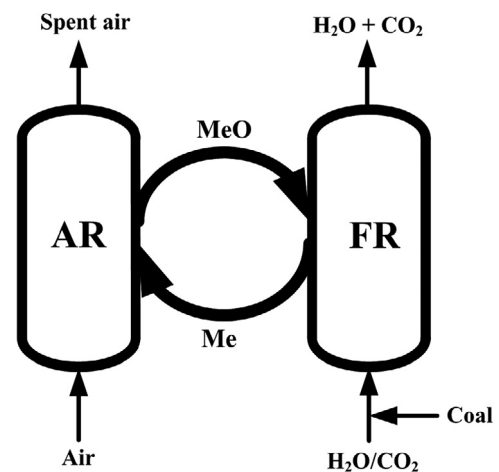

Fig. 1. General flow path of *i*G-CLC process.

environmentally benign and of low cost. In the last few decades, over 1000 kinds of OCs have been manufactured and tested under conditions of thermogravimetric analyzer (TGA), laboratory fluidized bed reactors as well as pilot scale chemical looping units, which have been comprehensively reviewed in Ref. [13]. During the early stage of CLC, materials for OC preparation were mostly pure chemicals, which exhibited the defect of high cost for industrial application. Additionally, due to the coal ash deposition, OC contamination by pollutants and materials loss in OC/ash separation process, the life cycle of the OC can be further reduced when being applied to coal-derived CLC process. Recently, increasing interests are being shown in natural minerals, *e.g.*, iron ore [15–21], copper ore [22–27] and manganese ore [28–31], which have been investigated and proposed to be possible OC candidates in chemical looping processes.

Iron ore, with the main active phase of Fe_2O_3, has been considered as a suitable OC option for coal-derived CLC process. However, the common weaknesses of Fe-based OCs are the low oxygen donating capacity and inferior CH_4 conversion efficiency [13]. Furthermore, the conversion rate of iron ore towards fuel gas is not sufficient high, which eventually needs the increase of OC circulation rate in CLC reactors to achieve satisfactory fuel conversion. Efforts have been done to improve the performance of iron ore OC via introducing foreign ions. Sun et al. [21] tried to improve the reactivity of a kind of Canadian ilmenite by coating with CeO_2, ZrO_2, NiO or Mn_2O_3. Both temperature-programmed CH_4 reduction tests and cyclic isothermal redox experiments (with CH_4 as fuel gas) in TGA demonstrated that the introduction of these metal oxides can either accelerate CH_4 conversion or enhance anti-sintering property of the OCs. Bao et al. [32] prepared three kinds of ilmenite OC by impregnating the raw ilmenite with K_2CO_3, Na_2CO_3 or $Ca(NO_3)_2$. They observed that the reactivity of the modified ilmenite with 15 wt% K^+ introduction can be improved ∼ 8 times faster than the raw activated ilmenite, and the reactivity enhancement was explained due to the improved porous structure induced by the migration of alkali ions. Gu et al. [16] investigated a kind of potassium improved iron ore OC in a laboratory-scale fluidized bed reactor, using anthracite as fuel. It was found that the addition of potassium can promote the carbon gasification and water-gas shift reaction significantly. Nevertheless, sintering on the surface of K_2CO_3-decorated iron ore particles was observed, which indicated that the K_2CO_3 loading ratio should be controlled at particularly low value. Yang et al. [14] proposed to modify hematite with Cu impregnation and the Cu loading ratio was optimized at 6 wt% by experiments in a batch fluidized bed reactor. As concluded, Cu-modified hematite showed much better reactivity towards coal gasification products than pure hematite.

Compared with iron ore, copper ore is relatively less investigated. A distinguished property of Cu-based OC is its capability of releasing gaseous oxygen under suitable conditions, which makes it possible for solid fuel to react directly with gaseous O_2 in chemical looping process, known as CLOU. Zhao et al. [23] investigated the performance of a kind medium Cu content (44.4 wt%) copper ore in anthracite-derived CLOU process. Typical high combustion efficiency (>96%) and CO_2 yield value (>0.95) were attained, and only slight sintering and agglomeration phenomenon was observed in the long-term test at 950 °C. Wang et al. [24] further studied the reactivity of the same copper ore OC with diverse ranks of coal (GP anthracite, FG bituminous and SL lignite) in a batch fluidized bed reactor. It was found that both the increase of reaction temperature and the decrease of coal rank can be beneficial for carbon conversion. The introduction of coal gasification agent (steam or CO_2) into the fuel reactor can improve the instantaneous char conversion rate of anthracite. A great challenge for applying copper ore in CLOU process is the sintering problem at high temperature, which should be carefully addressed. Three different natural copper ore particles with different CuO contents have been systematically tested in both TGA and fluidized bed reactor by Wen et al. [22]. The results indicated that agglomeration phenomenon did not occur to copper ore particles with a low CuO content (5.82 wt%) after 20 cycles at 980 °C. To improve the anti-sintering property of copper ore OC, calcium aluminate cement was adopted to mix with fine copper ore particles [26]. As observed, the OC with 20 wt% of cement loading showed the best redox reactivity and no tendency towards agglomeration was detected after 10 cycles in fluidized bed reactor at 950 °C with lignite as fuel.

As can be seen from the literatures review above, both iron ore and copper ore can be used as promising OC candidates in chemical looping processes. Copper ore shows high reactivity and oxygen decoupling property, but is prone to sintering at high temperatures

(>950 °C). Iron ore is favored for its low price and good recyclability in long-term redox tests, but is criticized for the inferior reactivity. It is well acknowledged that bimetallic oxides may exhibit better reactivity than single active phase oxides due to the potential synergistic effect. Performance of synthetic Cu-Fe bimetallic OC has been extensively evaluated in literatures [33–37], synergistic effect and improved reactivity was observed. Wang et al. [35] first synthesized the $CuFe_2O_4$ OC using a sol-gel combustion synthesis method, which integrated Fe and Cu metals into one oxide matrix. Reactivity of the $CuFe_2O_4$ OC towards coals was tested by TGA coupled Fourier transform infrared spectrometry (FTIR), and the results indicated that the bimetallic OC exhibited superior properties over single metal oxide of either Fe_2O_3 or CuO. Siriwardane et al. [36] came up with a kind of CuO-Fe_2O_3 mixed oxide OC for coal and methane CLC process. It was found that the obtained bimetallic OC can not only improve the oxygen release property of CuO, but also increase the reduction extent of Fe_2O_3 in both methane and coal. The synergistic reactivity of the CuO-Fe_2O_3 OC was explained due to the high dispersion of CuO and Fe_2O_3 species in the $CuFe_2O_4$ matrix. Yang et al. [38] adopted a mixture of well-sieved copper ore and hematite as OC in coal-derived CLC process, synergistic effect was observed between the mixed ore particles. The mixing OC with 20 wt% of copper ore showed much better reactivity towards coal gasification products than that of pure hematite, and much higher coal conversion rate was attained. However, segregation phenomenon may occur to the physically mixed ore particles when they are fluidized in CLC reactors, due to the different densities of copper ore and hematite. The use of cement as inert binder for OC preparation has been verified as a perfect way to recycle waste fine OC materials as well as to address the sintering issue of OCs [26,39,40]. In this work, waste fine particles (<0.1 mm) of hematite and copper ore after sieving were reused by cement bonding to produce bimetallic OC with relatively high disperse structure and good mechanical strength. The obtained OC is expected to integrate the merits of monometallic oxides to achieve possible synergistic reactivity in a single particle. Redox tests in both TGA and batch fluidized bed reactor were conducted to evaluate the reactivity and physical stability of the newly proposed OCs.

2. Experimental section

2.1. OC preparation

Waste fine particles (<0.1 mm) of natural copper ore and hematite, which are not suitable to be cyclically fluidized in CLC reactor, are reused by physically mixing with calcium aluminate cement to produce bimetallic OC with relatively high disperse structure and good mechanical strength. As obtained from X-ray fluorescence (XRF, EDAX EAGLE III) analysis together with the X-ray diffraction (XRD, X'Pert PRO) pattern, chemical compositions of the copper ore and hematite are presented in Table 1. Calcium aluminate cement is a kind of commonly used construction material, which mainly contains 44.0 wt% Al_2O_3, 38.9 wt% CaO and 10.3 wt% SiO_2, as declared by the production company. In this work, mixtures with different mass ratios of copper ore to hematite (i.e., 0/100, 10/90,

Table 1
Chemical compositions of natural copper ore and hematite.

Copper ore (wt.%)		Hematite (wt.%)	
CuO	21.04	Fe_2O_3	87.24
$CuFe_2O_4$	70.05	SiO_2	7.83
SiO_2	5.53	Al_2O_3	3.85
$CaSO_4$	2.29	Others	1.08
Al_2O_3	1.08	–	–

Table 2
Proximate and ultimate analyses of SL lignite and GP anthracite.

Coal type	Proximate analysis (wt.%, ad)				Ultimate analysis (wt.%, daf)				
	M	V	A	FC	C	H	O[a]	N	S
SL	8.62	41.59	35.47	14.32	48.33	4.11	2.14	0.85	0.48
GP	2.25	10.69	20.62	66.44	70.04	3.54	0.41	1.90	1.24

[a] Oxygen to balance.

20/80 ..., 100/0) were further mixed with cement (accounted for 20 wt% in the well-prepared OC), labeled as Fe100@C, Cu10Fe90@C, Cu20Fe80@C, ..., Cu100@C, respectively. After intensive mixing of the fine particles, deionized water was introduced to the mixtures and the obtained slurry was then electrically stirred well to ensure uniform distribution of the powders. The hardening process of the obtained paste occurred gradually at room temperature for 10 days. After which, the hardened mixtures were heat treated in a muffle oven at 500 °C for 5 h and then at 1000 °C for 10 h. Finally, particles after calcination were crushed and screened to the size range of 0.1–0.3 mm.

2.2. Fuel used

Simulated coal-derived synthesis gas, which contains 25 vol% H_2, 35 vol% CO and 40 vol% CO_2, was adopted as fuel gas in TGA experiments. Coal samples used in fluidized bed tests were Shengli (SL) lignite and Gaoping (GP) anthracite from China, which have been frequently studied in our group [24,26,27]. Apparent water in coal was removed by drying in a vacuum drying oven for 10 h at 105 °C, particles in the size range of 0.2–0.3 mm were screened out for use. Proximate and ultimate analyses of SL lignite and GP anthracite are shown in Table 2.

2.3. Experiments in TGA and fluidized bed reactor

Cyclic isothermal reduction-oxidation experiments of all the prepared OCs were carried out in TGA (WCT-1D, with a measurement precision of 1 μg) at 950 °C to optimize the copper ore to hematite mixing ratio. In each test, synthesis gas was used as fuel gas in the reduction stage for 6 min and air was employed as oxidizing agent in the oxidation stage for 6 min. To prevent the mixing of air and synthesis gas, N_2 was introduced as purging gas for 4 min between the oxidation stage and reduction stage. The gas flow rate in each stage was always controlled at 60 mL·min^{-1} by mass flow meter/controller and the sample mass in each test was approximate 20 mg. 11 redox cycles have been conducted for each OC sample.

Subsequently, the OC particles with an optimum copper ore to hematite mixing ratio were further tested in a batch fluidized bed reactor at 950 °C, using SL lignite and GP anthracite as fuels. 30 redox cycles were conducted to validate both the chemical reactivity and physical stability of the OCs. Gas mixture of high purity N_2 balanced steam was used as fluidization agent in the OC reduction stage, while air was adopted in the OC regeneration stage. To blow out the gaseous products, N_2 was introduced to purge the

reactor after each reduction stage. The gas flow rate in both reduction stage and oxidation stage was always set at 900 mL·min^{-1}, which corresponds to about 4–7 times of the minimum fluidization velocity of the particles. Certain amount of OC samples (40 g for Cu20Fe80@C and 47 g for Fe100@C, respectively, to guarantee the same amount of active lattice oxygen) was added into the reactor, exposing to air at a pre-set temperature for 30 min to ensure fully oxidation. When the desired temperature was achieved and stabilized, a batch of 0.35 g SL lignite (0.24 g for GP anthracite) was quickly introduced into the reactor. At this point, the oxygen to fuel ratio, Ω, for both OCs were determined as 2.0. We should note here that the determination of $\Omega = 1.0$ was on the basis of being Fe100@C reduced to Fe_3O_4, while Cu20Fe80@C to Cu_2O and Fe_3O_4. The experimental conditions are shown in Table 3, and each test has been repeated at least 3 times for accuracy concern.

A schematic layout of the fluidized bed reactor unit is shown in Fig. 2. The reactor system can be mainly divided into three parts, *i.e.*, gas supplying unit, reaction chamber and gas detecting unit. Air or N_2/H_2O can be introduced into the reaction chamber by the gas supplying unit to simulate the reaction atmosphere of AR or FR. Steam was generated by heating certain amount of feed water provided by a water pump, using a heating sleeve with the temperature controlled at around 250 °C to prevent steam condensation. The reaction chamber is a straight stainless steel tube with 890 mm height and 26 mm inner diameter, which is electrically heated by a furnace. Exhaust gases from the reactor are first filtered to remove particulate matter and electrically cooled to eliminate water vapor, then introduced to an on-line gas analyzer (Gasboard Analyzer 3100) to determine the contents of CO_2, CH_4, CO, H_2 and O_2. To be noted, the CO_2, CH_4 and CO concentrations were determined by nondispersive infrared analysis (NDIR), with an accuracy of 1% FS) and H_2 by thermal gas conductivity (TCD, with an accuracy of 2% FS), while the O_2 concentration was determined by electron capture detector (ECD, with an accuracy of 2% FS). Moreover, the accuracy of the detection sensors involved in this work is listed in Table 4.

2.4. Data evaluation

For TGA experiments, the weight loss ratio of the OCs during the reduction stage with synthesis gas, X_r (wt.%), was calculated as [41],

$$X_r = \frac{m_0 - m}{m_0} \times 100\% \tag{1}$$

Table 3
Experimental conditions of the batch fluidized bed tests.

|	OC type	Coal type	Coal feeding amount (g)	Ω (–)	Fluidization agent	Cycle number (–)
Case 1	Fe100@C	SL	0.35	2.0	50% H_2O + 50% N_2	3
Case 2	Cu20Fe80@C	SL	0.35	2.0	50% H_2O + 50% N_2	3
Case 3	Cu20Fe80@C	SL	0.35	2.0	40% H_2O + 60% N_2	3
Case 4	Cu20Fe80@C	SL	0.35	2.0	60% H_2O + 40% N_2	3
Case 5	Cu20Fe80@C	SL	0.70	1.0	50% H_2O + 50% N_2	3
Case 6	Cu20Fe80@C	SL	0.23	3.0	50% H_2O + 50% N_2	3
Case 7	Cu20Fe80@C	GP	0.24	2.0	50% H_2O + 50% N_2	3
Cyclic test 1#	Fe100@C	SL	0.35	2.0	50% H_2O + 50% N_2	30
Cyclic test 2#	Cu20Fe80@C	SL	0.35	2.0	50% H_2O + 50% N_2	30
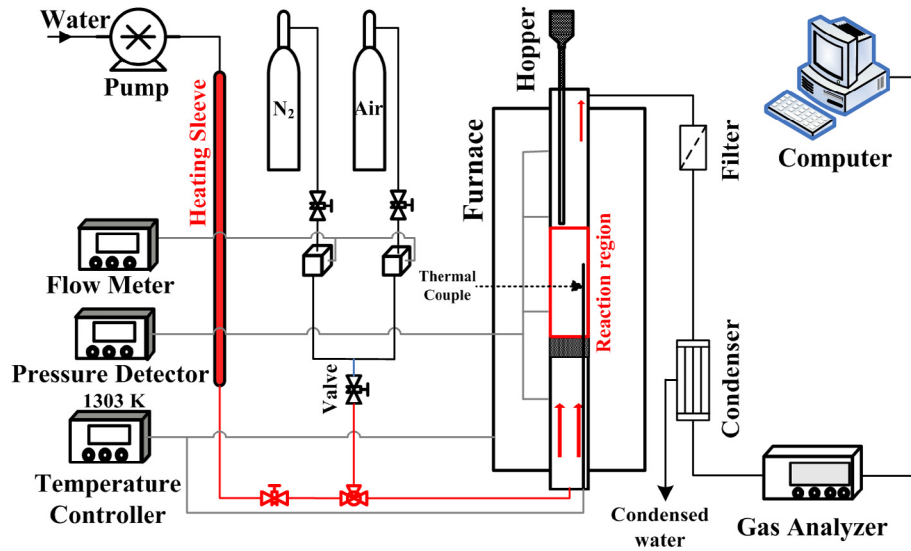
Fig. 2. Schematic layout of the fluidized bed reactor unit.

Table 4
The experimental sensors and uncertainties.

Items	Parameter range	Uncertainties
TGA-weight	1–300 mg	±1 μg
TGA-temperature (°C)	20–1500	±2.5
Fluidized bed reactor-temperature (°C)	20–1050	±5
CO_2 detector (vol.%)	0–100	±1
CH_4 detector (vol.%)	0–10	±0.1
CO detector (vol.%)	0–10	±0.1
H_2 detector (vol.%)	0–10	±0.2
O_2 detector (vol.%)	0–10	±0.2

The oxygen carrying capacity, R_o (–), was defined as [41],

$$R_o = \frac{m_o - m_r}{m_0} \times 100\% \tag{2}$$

where m_o (mg) and m_r (mg) are the weight of the OC at fully oxidized state and reduced state, respectively; m is the instantaneous weight of the OC at time t, mg; while m_0 is the weight of the OC at the beginning, mg.

To further investigate the OC reactivity in TGA experiments, the weight loss rate of OCs within the reduction stage, x_r (s^{-1}), was calculated as [26],

$$x_r = \frac{dX_r}{dt} \tag{3}$$

For fluidized bed experiments, as no carbonaceous gas was detected during air oxidizing stage, it was considered that carbon deposition phenomenon did not occur on the surface of OC particles within the OC reduction stage. In this sense, the carbon conversion, X_c (–) and gas yield of i (CO_2, CO and CH_4), γ_i (–), can be calculated as [42],

$$X_c = \frac{\int_{t_0}^{t} F_{out,red} \cdot \left(y_{CO_2} + y_{CO} + y_{CH_4}\right) dt}{\int_{t_0}^{t_{total}} F_{out,red} \cdot \left(y_{CO_2} + y_{CO} + y_{CH_4}\right) dt} \tag{4}$$

$$\gamma_i = \frac{\int_{t_0}^{t_{total}} \left(F_{out,red} \cdot y_i\right) dt}{\int_{t_0}^{t_{total}} F_{out,red} \cdot \left(y_{CO_2} + y_{CO} + y_{CH_4}\right) dt} \tag{5}$$

To evaluate the reactivity of OC with H_2, the yield of H_2 to total carbonaceous gas products was also determined [38],

$$\gamma_{H_2/C} = \frac{\int_{t_0}^{t_{total}} \left(F_{out,red} \cdot y_{H_2}\right) dt}{\int_{t_0}^{t_{total}} F_{out,red} \cdot \left(y_{CO_2} + y_{CO} + y_{CH_4}\right) dt} \tag{6}$$

where $F_{out,red}$ ($mL \cdot s^{-1}$) is the outlet gas flow rate (dry basis) at each second during the OC reduction stage, as calculated based on N_2 balance [38],

$$F_{out,red} = \frac{F_{N_2}}{1 - y_{CO_2} - y_{CO} - y_{CH_4} - y_{H_2} - y_{O_2}} \tag{7}$$

here, y_{CO2}, y_{CO}, y_{CH4}, y_{H2} and y_{O2} are the instantaneous volume fraction of CO_2, CO, CH_4, H_2 and O_2 in the flue gas (–), respectively; t_0 (s) and t_{total} (s) represent the time points of the start and the end of the reduction stage, respectively; F_{N2} is the inlet flow rate of N_2, $mL \cdot s^{-1}$.

To further investigate the OC reactivity with coal, the carbon conversion rate, x_c (s^{-1}), was calculated [24],

$$x_c = \frac{dX_c}{dt} \tag{8}$$

Then, the instantaneous carbon conversion rate, x_{inst} (s^{-1}), based on the remaining unreacted carbon, was calculated as [24],

$$x_{inst} = \frac{1}{1 - X_c} \frac{dX_c}{dt} \tag{9}$$

3. Results and discussions

3.1. OC optimization in TGA

Cyclic isothermal redox experiments of the OCs with synthesis gas as reducing agent and air as oxidizing agent were first conducted at 950 °C in TGA. Fig. 3 shows the weight loss ratio of the OCs within the N_2 purging stage and synthesis gas reducing stage at the 10th cycle. As it can be seen, there shows an obvious slow mass decreasing trend during the N_2 purging stage for OC samples with copper ore addition, which is attributed to the decomposition of CuO (CuO → Cu_2O + O_2). After synthesis gas was introduced, weight of all samples decreased rapidly to relatively stable values within 90 s. Moreover, the final weight loss ratio of different samples varied, which increased nonlinearly with the increase of copper ore content in the OC. According to the chemical analysis of copper ore and hematite shown in Table 1, together with the weight loss ratio of the OCs shown in Fig. 3, it was observed that
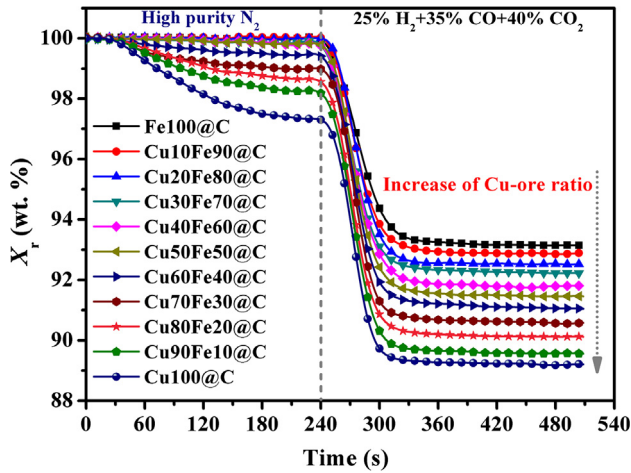
Fig. 3. Weight loss ratio of the OCs within the N_2 purging and synthesis gas reduction stages at the 10th cycle.

the reduced state of copper ore and hematite achieved in TGA was Cu/FeO and FeO, respectively. And this can be validated straightforwardly, which take Fe100@C and Cu100@C as examples: the theoretical weight loss ratio for Fe100@C being reduced to FeO is 6.98 wt% and for Cu100@C being reduced to Cu/FeO is 10.84 wt%; while the experimental values were 6.85 wt% and 10.75 wt%, respectively. From this perspective, the addition of cement showed little influence on the final reduced state of hematite or copper ore, i.e., not affecting the oxygen donating capacity of OCs. Actually, XRD patterns shown later also indicated that chemical combination between cement and the active phase in OCs did not occur.

To examine the cyclic stability in multi-cycle redox process, oxygen donating capacity of the OCs within 11 cycles were calculated, as shown in Fig. 4. Generally, rather stable oxygen donating capacity can be achieved after cycle 7 for all OC samples. Moreover, there shows an increasing trend of the oxygen donating capacity with the increase of copper ore content in the bimetallic OC. The result is to be expected, since larger amount of available active lattice oxygen is carried by per unit weight of copper ore than that of hematite. Moreover, when looking into the final stable oxygen donating capacity of different OCs, it is observed that the increase of oxygen donating capacity shows nonlinear relationship with the
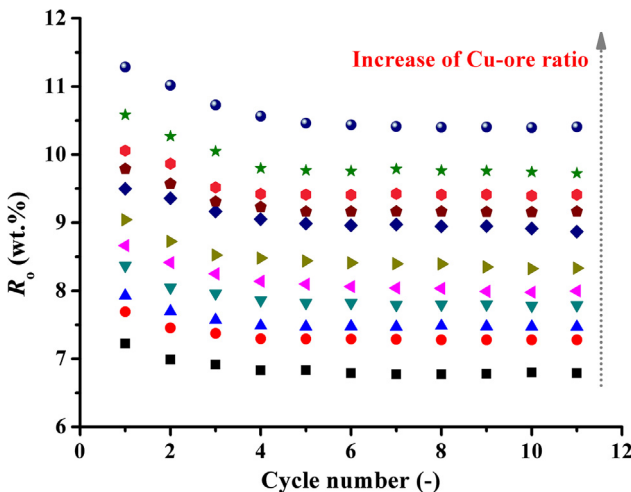
copper ore addition in the OC, especially for OCs with copper ore addition in the range of 0–20 wt%, 50–60 wt% and 90–100 wt%. This unusual phenomenon can be attributed to the synergistic effect between copper ore (CuO) and hematite (Fe_2O_3) [38].

In view of the fact that the OC reactivity tends to be stable after 7 redox cycles, experimental data of the OCs at the 10th cycle was then selected out to make a comparison. Fig. 5 shows the weight loss rate of the OCs as a function of time. To be noted, the much smaller weight loss rate of some OCs during the first 200 s was due to the oxygen release of copper ore, which has already been clarified in Fig. 3. As can be seen, the peak value of the weight loss rate generally increases with the copper ore loading ratio in the OC, in which Cu100@C shows the highest peak value while Fe100@C exhibits the lowest one. The reason is obvious: CuO has long been validated to exhibit much better reactivity than Fe_2O_3 in chemical looping processes [43]. Larger proportion of copper ore content in the bimetallic OC will ultimately contribute to higher reactivity. Nevertheless, it was found that the peak value of Cu20Fe80@C exceeded over Cu30Fe70@C and was nearly the same with that of Cu40Fe60@C. Moreover, the peak weight loss rate of Cu80Fe20@C and Cu90Fe10@C were closely equal to each other. At this point, synergistic effect between copper ore and hematite was validated again. Actually, repeated experiments have been performed to eliminate possibly existed experimental error. The results indicated that the experimental error was too small to affect the conclusion and synergistic effects between copper ore and hematite do exist. Clarification of the synergistic effect between copper ore and hematite can be found in our previous publication [38].

As known, the reaction of synthesis gas with CuO is exothermic, while with Fe_2O_3 is endothermic [44]. From this perspective, it is theoretically possible to achieve auto-thermal balance in FR by adjusting the mixing ratio of copper ore and hematite in the bimetallic OC. Once auto-thermal balance was attained, temperature in FR can be more easily controlled, which is then favorable for operational flexibility of the CLC unit. Fig. 6 shows the differential thermal analysis (DTA) results of the OCs during the reduction stage. For accuracy concern, the result shown here was an average value of the last three cycles for each OC. As seen, for OCs with copper ore loading ratio larger than 20 wt%, the reduction process was exothermic, and the heat release capacity of the OC increased gradually with the elevated copper ore loading ratio. To be noted, for Cu20Fe80@C and Cu10Fe90@C, the heat release/absorb during the reduction stage were both very close to zero, which have the potential to achieve auto-thermal balance in FR. However, when turn to industrial application, considering the inevitable heat leakage of the CLC reactor, the Cu20Fe80@C OC with slight exothermic characteristic could be more feasible to achieve auto-thermal balance.

As summarized from the results obtained in TGA, cement bonded fine hematite and copper ore particles performed well as OC with synthesis gas as fuel. Stable reactivity of the OCs could be attained after 7 redox cycles and synergistic effect between hematite and copper ore was also verified. It seems that the OC with larger proportion of copper ore exhibits much better reactivity. However, copper ore is more expensive than hematite, thus large copper ore loading ratio in the OC is economically unfavorable. Additionally, more copper ore addition means more CuO content, which is more easily to result in OC sintering/agglomeration problem [22]. Together with the concern that the OC with 20 wt % of copper ore addition could ultimately achieve auto-thermal balance in FR, Cu20Fe80@C is considered to be the most suitable OC candidate for industrial application. Further test of the Cu20Fe80@C OC was conducted in a batch fluidized bed reactor using coal as fuel.
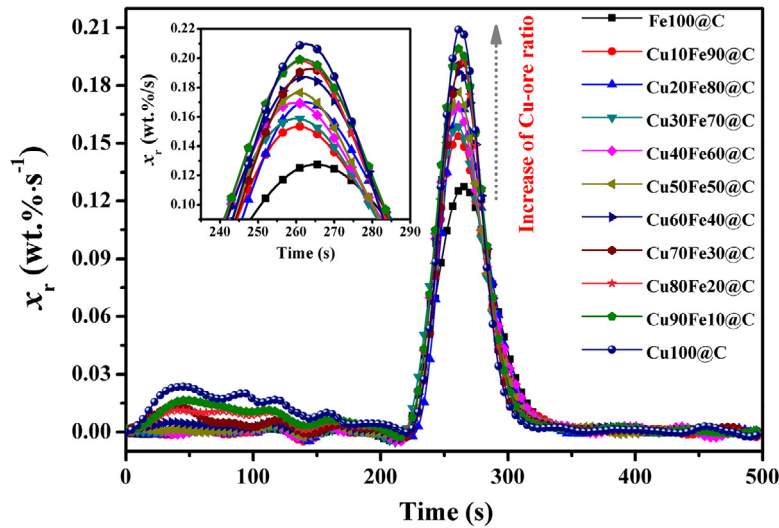

Fig. 4. Oxygen carrying capacity of the OCs vs. cycle numbers.

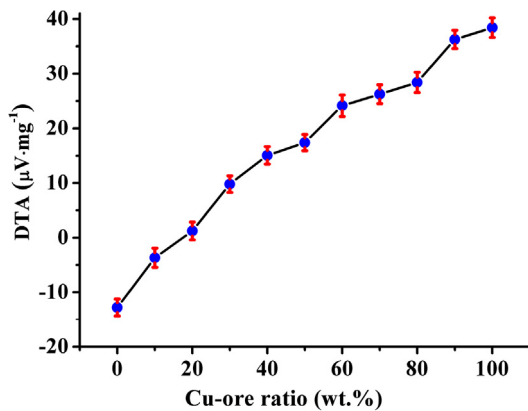**Fig. 5.** Weight loss rate of the OCs *vs.* time at the 10th cycle.

Fig. 6. DTA signal of the OCs with different Cu-ore addition ratios during the reduction stage.

3.2. Fluidized bed experiments

Fig. 7 compares the outlet gas concentrations in SL coal-derived iG-CLC process using Fe100@C and Cu20Fe80@C as OC, respectively. For each test, the reaction temperature was always maintained at 950 °C, the oxygen to fuel ratio was set at 2.0 and 900 mL·min^{-1} of 50 vol% H_2O + 50 vol% N_2 was used as the fluidization agent. Generally, the exhaust gas concentration profiles show

rather similar trend for the two kind of OCs. Most of the combustible contents in coal were fully converted into CO_2 and H_2O by the OC. During the fast coal pyrolysis stage, small proportion of reducing gas (mainly of CO and H_2, almost no CH_4) ran away from the reactor without being oxidized. Subsequently, the remaining coal char was gradually gasified by steam and the generated gasification products were further oxidized by OC particles, which contributed to the peak value of CO_2 concentration. Nevertheless, differences in gas evolution behavior were also observed when using the two OCs, which relatively higher CO_2 peak value as well as lower CO and H_2 peak values were attained for Cu20Fe80@C than those of Fe100@C. Additionally, the escape of unburned combustible gas (CO and H_2) from reactor lasted a much longer time for Fe100@C when compared with Cu20Fe80@C. In this sense, Cu20Fe80@C exhibited much better reactivity towards coal gasification products than that of Fe100@C in fluidized bed reactor. Therefore, performance of Cu20Fe80@C in iG-CLC process was further evaluated in following tests.

In coal-direct CLC process, the existence of gasification agent, *i.e.*, H_2O and CO_2 (especially H_2O), can greatly facilitate coal conversion [24,45]. Moreover, the different concentrations of gasification agent in fluidization gas may result in diverse coal conversion characteristic. Therefore, the effects of steam concentration on carbon conversion rate as well as gas yield within the iG-CLC process using Cu20Fe80@C as OC and SL coal as fuel were investigated, as shown in Fig. 8. The steam concentration varied from 40 to 60 vol%, the oxygen to fuel ratio was 2.0 and the reaction temperature was
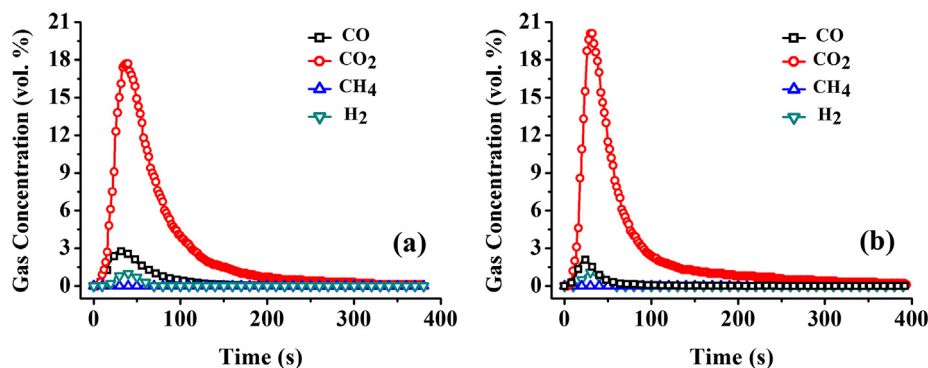

Fig. 7. Gas concentration profiles of (a) Fe100@C and (b) Cu20Fe80@C with SL coal. Reaction temperature: 950 °C. Steam concentration: 50 vol%. Oxygen to fuel ratio: Ω = 2.0.
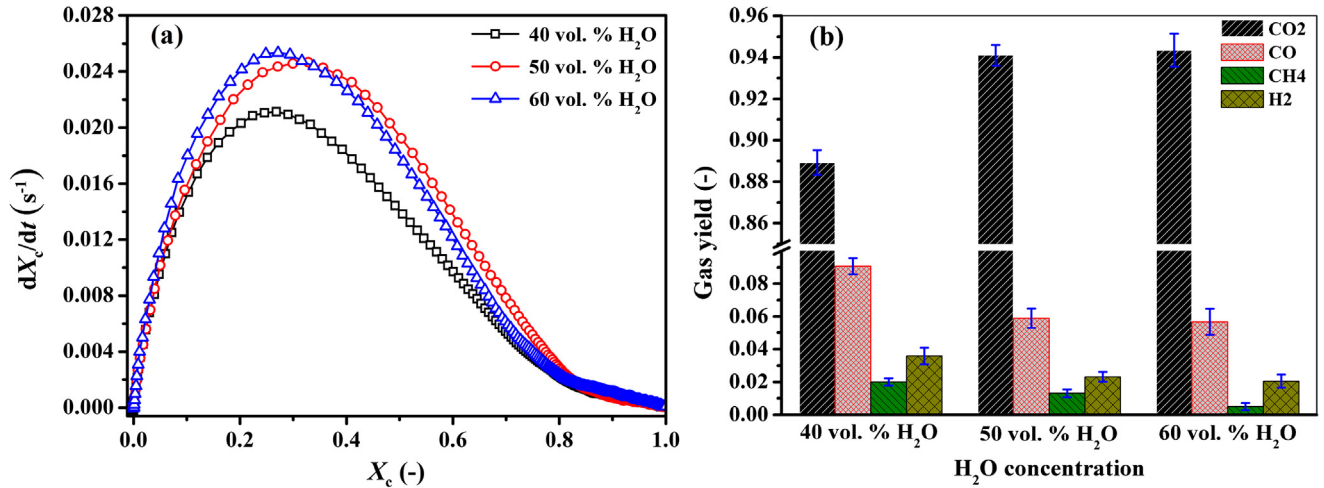
Fig. 8. Effect of steam concentration on (a) carbon conversion rate and (b) gas yield of Cu20Fe80@C with SL coal. Reaction temperature: 950 °C. Oxygen to fuel ratio: $\Omega = 2.0$.

maintained at 950 °C. As presented in Fig. 8a, the carbon conversion rate as a function of carbon conversion accelerated a lot with the steam concentration increased from 40 vol% to 50 vol%, while further increase of the steam concentration to 60 vol% did not change a lot. Similar phenomenon was also observed for the gas yield result. As can be seen, the CO_2 yield increased from 0.89 at 40 vol% steam concentration to 0.94 at 50 vol% steam concentration, yet no further increase from 50 vol% to 60 vol% was observed. The results indicated that a higher steam concentration could promote the coal conversion process and result in much higher CO_2 yield. Nevertheless, it does not mean that the higher steam concentration the better. Higher steam concentration means larger thermal input for steam generation and more heat loss in the final condensation process for CO_2 purification. Additionally, considering that SL lignite is relatively easy to be gasified and further increase of steam concentration from 50 vol% to 60 vol% does not result in much better reactivity significantly, thus 50 vol% of steam in fluidizing gas is enough already.

Fig. 9a and b presents the effects of oxygen to fuel ratio on carbon conversion and gas yield for Cu20Fe80@C sample with SL lignite. The reaction temperature was kept at 950 °C and the fluidization gas was 900 mL·min^{-1} of 50 vol% H_2O + 50 vol% N_2. The different oxygen to fuel ratio was realized by adjusting the coal

feeding amount in each test. As seen, the increase of oxygen to fuel ratio generally poses positive effects on coal conversion. Both the carbon conversion and CO_2 yield increased significantly from $\Omega = 1.0$ to $\Omega = 2.0$. The reason is obvious: larger oxygen to fuel ratio means relatively higher OC inventory to convert per unit fuel. In other words, more active lattice oxygen is available for fuel conversion, which eventually contributes to much faster carbon conversion. However, as the oxygen to fuel ratio increased from $\Omega = 2.0$ to $\Omega = 3.0$, the enhancement of CLC performance was not so obvious. This behavior may be attributed to the limitation of the slow coal/char gasification process. Moreover, the yield of unburned gas showed a decreasing trend with the increase of oxygen to fuel ratio. From this perspective, the larger oxygen to fuel ratio could be beneficial for SL lignite conversion in iG-CLC process. However, we should also note here that smaller oxygen to fuel ratio can reduce OC inventory, so as to realize compact reactor design and less capital investment. In this sense, balance between fuel conversion characteristic and oxygen to fuel ratio should be comprehensively evaluated when turning to industrial application.

Effect of coal type on the performance of Cu20Fe80@C OC was also evaluated. Fig. 10 shows the carbon conversion and instantaneous carbon conversion rate of Cu20Fe80@C OC with SL lignite and GP anthracite. The reaction temperature was 950 °C, the
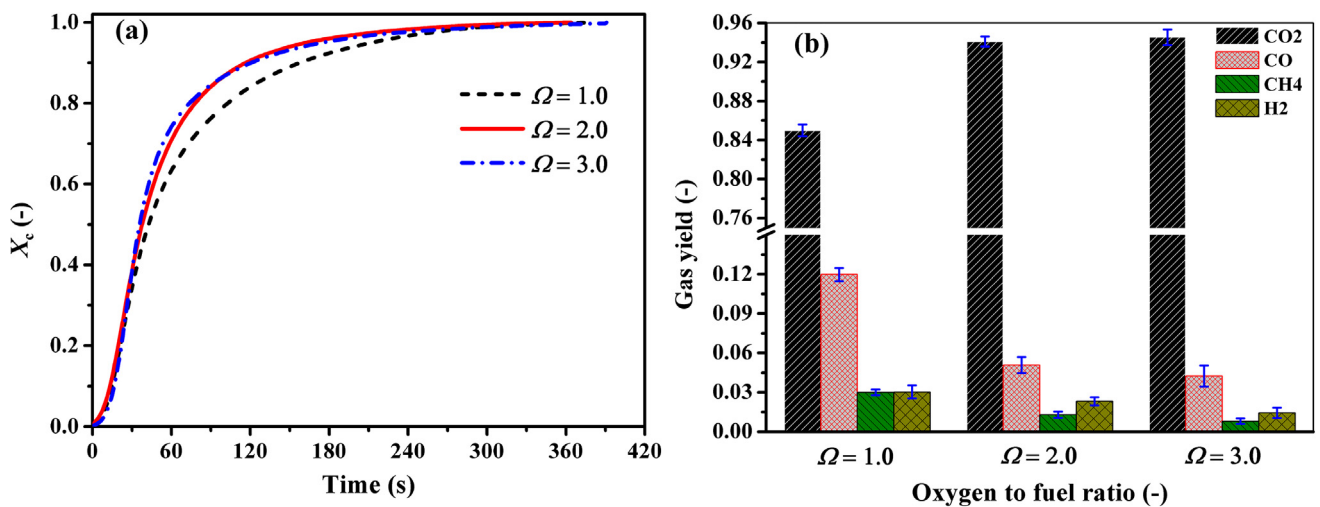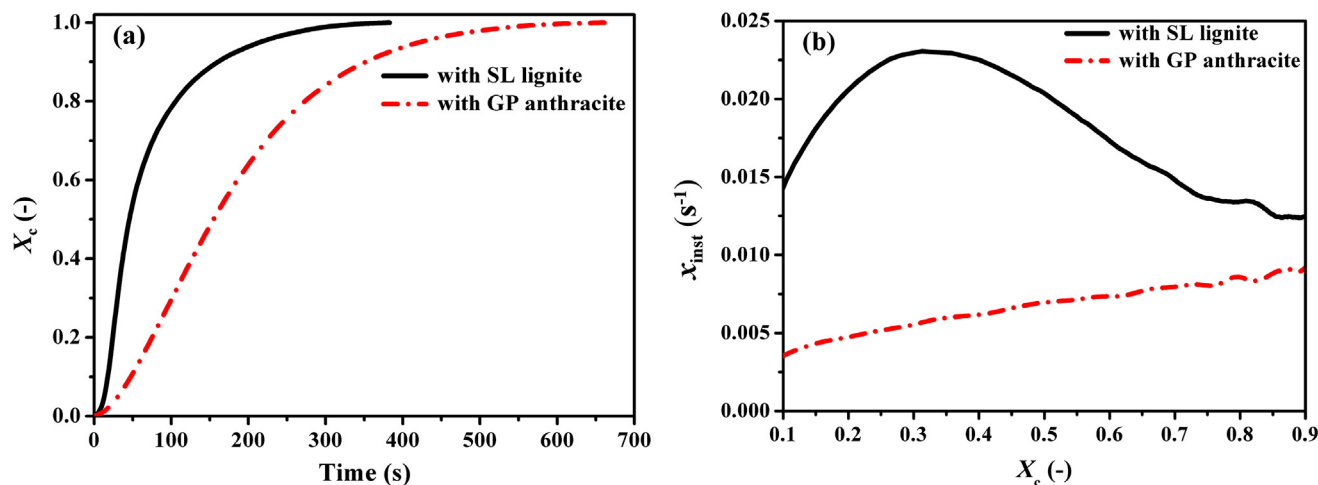

Fig. 9. Effect of oxygen to fuel ratio (Ω) on (a) carbon conversion and (b) gas yield of Cu20Fe80@C with SL coal. Reaction temperature: 950 °C. Steam concentration: 50 vol%.

Fig. 10. Carbon conversion *vs.* time and instantaneous rate of carbon conversion *vs.* carbon conversion using SL and GP coal for Cu20Fe80@C. Reaction temperature: 950 °C. Steam concentration: 50 vol%. Oxygen to fuel ratio: Ω = 2.0.

oxygen to fuel ratio was 2.0 and 900 mL·min^{-1} of 50 vol% H_2O + 50 vol% N_2 was used as fluidization agent. The difference of using lignite and anthracite as fuel with Cu20Fe80@C OC was obvious. As presented in Fig. 10a, SL lignite can achieve complete conversion in less than 400 s, while over 650 s is required for GP anthracite. Additionally, comparison of the instantaneous carbon conversion rate between the two coals, as shown in Fig. 10b, further illustrates the better conversion characteristic of Cu20Fe80@C OC with SL lignite. The main reason for the aforementioned difference can be attributed to the different gasification characteristic of the two coals, which lignite can be more easily gasified by H_2O than anthracite. As gasification is the limitation step in the *i*G-CLC process of coal, it is no wonder that much better combustion characteristic was attained when using lignite as fuel. Actually, previous publication [24] also demonstrated that lignite is both economically and technically feasible to be converted by Fe-based OC in *i*G-CLC process.

To further investigate the cyclic reactivity of the proposed OC in *i*G-CLC process, 30 cyclic redox tests with SL lignite have been conducted for Cu20Fe80@C as well as Fe100@C. Fig. 11 shows the gas yield of CO_2, CO, CH_4 and H_2 for both OCs within 30 cycles. For all tests, the reaction temperature was controlled at 950 °C, the flu-

idization agent was 900 mL·min^{-1} of 50 vol% H_2O + 50 vol% N_2 and the oxygen to fuel ratio was always maintained at 2.0. As seen, relatively stable gas yield result can be attained after 10 cycles for both Cu20Fe80@C and Fe100@C. Moreover, the CO_2 yield of Cu20Fe80@C was always higher, while gas yield of CO, CH_4 and H_2 were lower than Fe100@C in each cycle. The results shown in Fig. 11 illustrate that both cement bonded fine particles exhibit stable reactivity in *i*G-CLC and better reactivity of Cu20Fe80@C than Fe100@C is further validated in cyclic fluidized bed experiments.

3.3. OC characterization

Fig. 12 shows the XRD patterns (Cu Kα radiation, accelerating voltage of 40 kV and tube current of 40 mA) of the fresh (in oxidation state) and used (in reduction state) OC samples with SL coal after 30 redox cycles in fluidized bed reactor. As seen, the active component of fresh Fe100@C OC is mainly Fe_2O_3, while the fresh Cu20Fe80@C sample contains Fe_2O_3, CuO and $CuFe_2O_4$. As the OC inventory was a little excessive to fully convert the coal (Ω = 2.0) in cyclic fluidized bed experiments, small proportion of Fe_2O_3 was detected in the used particles for both OCs. Note that, a phase of $Ca_2Al_2SiO_7$ (named gehlenite) was formed in the two cement bonded OCs according to the combination reaction among CaO, Al_2O_3 and SiO_2, which are the main contents of calcium aluminate cement. Moreover, the $Ca_2Al_2SiO_7$ phase remained unchanged before and after being tested in fluidized bed experiments, and chemical interaction among the cement contents and the active phase of OC did not occur, which indicated that the formed $Ca_2Al_2SiO_7$ was relatively stable in the OC. Actually, the melting point of $Ca_2Al_2SiO_7$ is 1584 °C [39], which acted as a perfect inert support in the OC, and this can explain the good anti-sintering property of cement bonded OCs in fluidized bed experiments.

The morphological and structural changes of the used Fe100@C and Cu20Fe80@C OC samples were analyzed by environmental scanning electron microscope (ESEM, FEI Quanta 200), with the accelerating voltage of 20.0 kV. Two magnification levels (500× and 1000×) were chosen for both OCs. Moreover, ESEM coupled energy dispersive X-ray spectroscopy (EDX) was employed to investigate the element distribution on the surface of used OC particles, as shown in Fig. 13. With respect to the surface morphology of used particles, both Fe100@C and Cu20Fe80@C display rather rough and porous structure, which could be beneficial for the OC reactivity. Sintering phenomenon was not observed on the surface
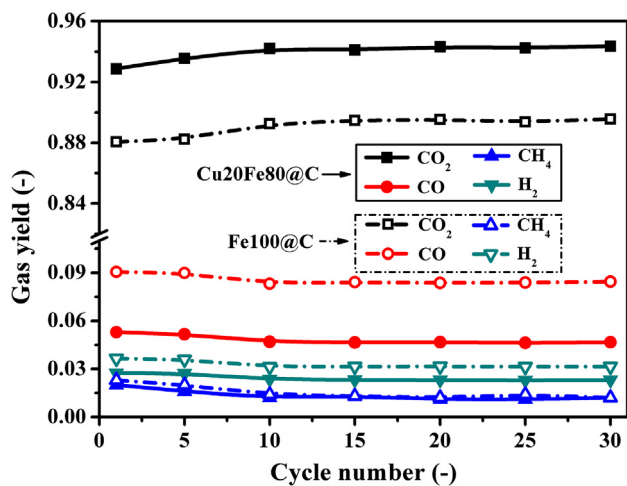
Fig. 11. Gas yield of CO_2, CO, CH_4 and H_2 for the OC samples of Fe100@C and Cu20Fe80@C with SL coal during 30 redox cycles. Reaction temperature: 950 °C. Steam concentration: 50 vol%. Oxygen to fuel ratio: Ω = 2.0.
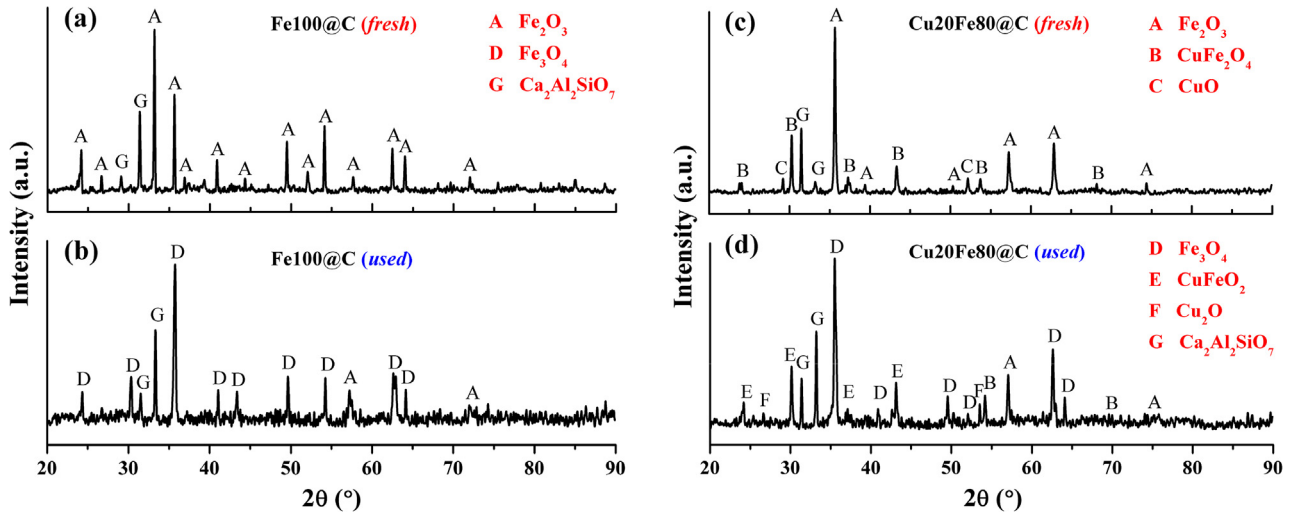
Fig. 12. XRD results of fresh Fe100@C (a) and Cu20Fe80@C (c); reduced Fe100@C (b) and Cu20Fe80@C (d) with SL coal after 30 redox cycles in fluidized bed reactor.
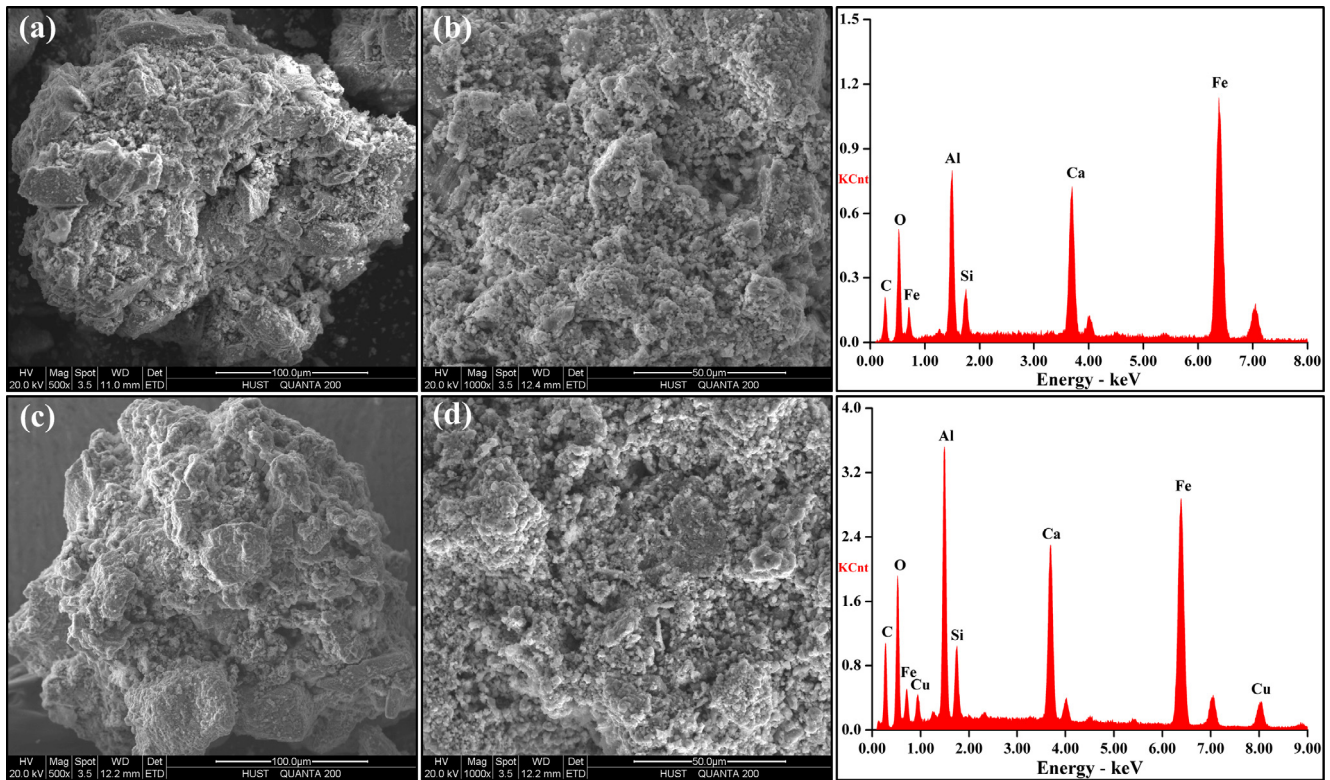

Fig. 13. ESEM images and EDX analyses of reduced Fe100@C (a, b) and Cu20Fe80@C (c, d) with SL coal after 30 redox cycles in fluidized bed reactor. Magnification of 500× for a, c and 1000× for b, d.

of both OC particles, this can be mainly attributed to the sintering inhibition effect of cement in the OC [26,39]. The EDX results show that Fe, Ca, Si, Al, Mg, O and C were detected in both OC, while Cu was only detected in Cu20Fe80@C. To be noted, the detected C was derived from carbon coating on the particles (to enhance the electrical conductivity of the particles) before the ESEM tests. Moreover, typical coal ash content (Na, K, et al. [22]) was not detected on the surface of the used OC particles, which indicated that ash deposition did not occur on the surface of OCs during the coal-derived iG-CLC process. The crushing strength (an average value of 25 measurements) of both the fresh and used OCs were measured by a digital dynamometer (Shimpo, FGP-100), with values

of 1.8 (±0.2) N and 2.1 (±0.1) N for fresh Fe100@C and Cu20Fe80@C, respectively; while 1.9 (±0.1) N and 2.3 (±0.2) N for used Fe100@C and Cu20Fe80@C, respectively. The results indicated that the OCs exhibit sufficient hardness to be fluidized in CLC reactor [46].

3.4. Discussions

The use of copper ore, iron ore, mechanically-mixed copper and iron ores as well as cement-decorated copper ore as OC in coal-derived chemical looping process have been demonstrated in our previous publications [26,38]. Synergistic effect was observed between iron ore and copper ore [38], where the bimetallic

Cu-Fe OC was produced by physically mixing well-sieved copper ore and iron ore particles (0.18–0.28 mm) according to the preset mixing ratios. In this way, the iron ore and copper ore contents of the obtained OC were independently existed in particle scale. As the densities of copper ore and iron ore were different from each other (5353 kg·m^{-3} for copper ore and 3742 kg·m^{-3} for iron ore), when the bimetallic OC particles were fluidized in CLC reactor, the OC particles would stratified along the bed height. While in this work, fine particles (<0.1 mm) of copper ore and iron ore were combined together by the addition of cement, which ultimately led to the coexistence of copper ore and iron ore contents in a single particle. In this sense, particle segregation phenomenon can be avoided and synergistic effect is ultimately achieved by this combination. From this perspective, it is no wonder for the much higher instantaneous carbon conversion rate attained for the Cu20Fe80@C OC in this work than that of the 2Cu8Hem OC (mixture of copper ore (20 wt%) and iron ore (80 wt%)) in Ref. [38], both using GP anthracite as fuel.

When comparing with the results obtained in Ref. [26], where experiments of copper ore and cement-decorated copper ore with SL coal were conducted, the Cu20Fe80@C OC was also favored for its high reactivity, even though its lattice oxygen content was relatively low. To be more specific, the peak values of carbon conversion rate for copper ore and Cu-C-20 (copper ore with 20 wt% of cement addition) obtained in previous research [26] were approximate 0.028 s^{-1} and 0.053 s^{-1} at the first cycle, respectively. While in this work, the Cu20Fe80@C OC can achieve a peak carbon conversion rate value as high as 0.025 s^{-1} within iG-CLC process. Note that, the carbon conversion rates for copper ore and Cu-C-20 showed a decreasing trend with cyclic number; while for Cu20Fe80@C OC, as depicted in Fig. 11, increased OC reactivity with cyclic number was observed. Additionally, for both Cu20Fe80@C and Cu-C-20, no sharp decrease of carbon conversion rate was observed at the late stage of coal conversion process when compared with that of pure copper ore.

Experimental results in this work also indicated much better reactivity of cement-modified iron ore than that of pure iron ore investigated in Ref. [38], which higher CO$_2$ yield was ultimately achieved. Together with the results obtained in Ref. [26], which enhanced reactivity of cement supported copper ore was achieved when compared with that of pure copper ore. The superiority of introducing cement into the OC preparation process was verified once again. The reasons for the enhanced reactivity of OC with cement addition can be two-fold: on the on hand, precursors (both cement and the ores) of the cement supported OCs were fine particles, much larger surface area of the obtained OC was achieved and eventually result in superior reactivity; on the other hand, the generated gehlenite phase during the calcination process of cement supported OCs could act as a inhibitor of OC sintering, which was beneficial to maintain the porous structure of the OC in cyclic redox tests. Note that, the calcium content in cement may act as catalyst for coal gasification in iG-CLC process, which may be another reason for the enhanced OC reactivity. Therefore, fundamental work is still necessary for comprehensive clarification of the improved reactivity of cement-decorated OC.

4. Conclusions

In this work, cement bonded fine hematite and copper ore particles are proposed as bimetallic OC in iG-CLC process. Experiments in both TGA and batch fluidized bed reactor were conducted to evaluate the OC performance, using synthesis gas and coal as fuels.

TGA results indicate that stable reactivity of the OCs can be achieved after 7 redox cycles, and the larger loading ratio of copper ore in the bimetallic OC generally leads to much higher oxygen donating capacity as well as better reactivity towards synthesis gas. Synergistic reactivity of the bimetallic OCs was achieved by the coexistence of copper ore and hematite in a single OC particle. Based on the considerations of OC reactivity, economic cost and auto-thermal balance in fuel reactor, the copper ore to hematite mixing ratio was optimized at 20:80 in weight, namely Cu20Fe80@C.

Subsequently, performance of the optimized Cu20Fe80@C OC was further evaluated in a batch fluidized bed reactor. It was found that the Cu20Fe80@C OC is more reactive to coal gasification products than that of Fe100@C, due to the synergistic effect achieved by the presence of copper ore and hematite contents in a single OC particle. The increase of steam concentration in fluidization agent as well as oxygen to fuel ratio can both accelerate the coal conversion rate of Cu20Fe80@C OC in iG-CLC process. Nevertheless, with concerns of the limited enhancing effect of too high of steam concentration or oxygen to fuel ratio, they are not the higher the better for economical operation in industrial units. Since higher steam concentration means higher thermal input for water evaporation and larger thermal loss in the flue gas condensation process for CO$_2$ purification. Moreover, higher oxygen to fuel ratio will lead to larger OC inventory, which is against the compact reactor design and economical operation. The coal rank was found to affect the performance of Cu20Fe80@C OC significantly, which the time duration for complete conversion was less than 400 s for lignite but over 650 s for anthracite. This can be mainly attributed to the different gasification reactivity of lignite and anthracite towards H$_2$O. Long term cyclic tests in fluidized bed reactor with lignite verified the superior reactivity of Cu20Fe80@C than that of Fe100@C, but nice fluidization behavior and good anti-sintering property were attained for both OCs. XRD analyses of the used samples validated that chemical combination between cement and the active phase in OCs did not occur. Moreover, ESEM images of the used particles showed that no obvious sintering phenomenon was observed, due to the sintering inhibition effect of cement.

The experimental results indicated that synergistic reactivity can be achieved when copper ore and hematite are coexisted in one particle, which ultimately contributes to superior anti-sintering property and improved reactivity of the bimetallic OC. Moreover, cement acts as a suitable inert support to bond fine ore particles for reutilization as OC and the existence of cement can be helpful for the stabilization of OC reactivity in cyclic redox processes. Considering that the raw OC materials were reutilized from waste fine hematite and copper ore particles, and the inert support of cement is quite cheap, together with the high reactivity of the bimetallic OC with lignite in iG-CLC process, the proposal of using cement bonded fine hematite and copper ore particles as OC could be rather competitive and promising in commercial application.

It should be noted that, the optimum copper ore to hematite mixing ratio attained in the present work was based on the specific copper ore and hematite that were frequently studied in our group. But we hold the view that synergistic reactivity may also be achieved when other similar copper ores and iron ores, even copper ores and manganese ores as well as iron ores and manganese ores were coexisted in one OC particle by cement bonding. Of course, the optimum mixing ratio should be re-determined accordingly. Generally, the loading ratio of the natural ore with better reactivity should be controlled in the range of 20–40 wt%, and the present study can offer a good example for the loading ratio optimization of different ingredients. Furthermore, a novel way for reutilization of waste fine OC particles (not only natural ores but also fine particles generated during fresh OC grinding or by OC abrasion in operation) by cement bonding was provided in this work, and the cement bonding can also be utilized to produce

bimetallic or even multi-metal oxides OCs with synergistic reactivity.

Acknowledgments

References

[1] Li F, Fan L. Clean coal conversion processes–progress and challenges. Energy Environ Sci 2008;1:248–67.

[2] Li B, Duan Y, Luebke D, Morreale B. Advances in CO_2 capture technology: a patent review. Appl Energy 2013;102:1439–47.

[3] Zhou W, Wang T, Yu Y, Chen D, Zhu B. Scenario analysis of CO_2 emissions from China's civil aviation industry through 2030. Appl Energy 2016;175:100–8.

[4] Li G, Liu D, Xie Y, Xiao Y. Study on effect factors for CO_2 hydrate rapid formation in a water-spraying apparatus. Energ Fuel 2010;24:4590–7.

[5] Li G, Zheng X. Thermal energy storage system integration forms for a sustainable future. Renew Sust Energ Rev 2016;62:736–57.

[6] Ishida M, Jin H. A new advanced power-generation system using chemical-looping combustion. Energy 1994;19:415–22.

[7] Lyngfelt A, Leckner B, Mattisson T. A fluidized-bed combustion process with inherent CO_2 separation; application of chemical-looping combustion. Chem Eng Sci 2001;56:3101–13.

[8] Leion H, Mattisson T, Lyngfelt A. The use of petroleum coke as fuel in chemical-looping combustion. Fuel 2007;86:1947–58.

[9] Siriwardane R, Tian H, Miller D, Richards G, Simonyi T, Poston J. Evaluation of reaction mechanism of coal–metal oxide interactions in chemical-looping combustion. Combust Flame 2010;157:2198–208.

[10] Bao J, Li Z, Cai N. Interaction between iron-based oxygen carrier and four coal ashes during chemical looping combustion. Appl Energy 2014;115:549–58.

[11] Lyngfelt A. Chemical-looping combustion of solid fuels–status of development. Appl Energy 2014;113:1869–73.

[12] Knutsson P, Linderholm C. Characterization of ilmenite used as oxygen carrier in a 100 kW chemical-looping combustor for solid fuels. Appl Energy 2015;157:368–73.

[13] Adanez J, Abad A, Garcia-Labiano F, Gayan P, de Diego LF. Progress in chemical-looping combustion and reforming technologies. Prog Energ Combust Sci 2012;38:215–82.

[14] Yang W, Zhao H, Ma J, Mei D, Zheng C. Copper-decorated hematite as an oxygen carrier for in situ gasification chemical looping combustion of coal. Energ Fuel 2014;28:3970–81.

[15] Xiao R, Song Q, Song M, Lu Z, Zhang S, Shen L. Pressurized chemical-looping combustion of coal with an iron ore-based oxygen carrier. Combust Flame 2010;157:1140–53.

[16] Gu H, Shen L, Xiao J, Zhang S, Song T, Chen D. Iron ore as oxygen carrier improved with potassium for chemical looping combustion of anthracite coal. Combust Flame 2012;159:2480–90.

[17] Gu H, Shen L, Zhong Z, Niu X, Liu W, Ge H, et al. Cement/CaO-modified iron ore as oxygen carrier for chemical looping combustion of coal. Appl Energy 2015;157:314–22.

[18] Ma J, Zhao H, Tian X, Wei Y, Zhang Y, Zheng C. Continuous operation of interconnected fluidized bed reactor for chemical looping combustion of CH_4 using hematite as oxygen carrier. Energ Fuel 2015;29:3257–67.

[19] Ma J, Zhao H, Tian X, Wei Y, Rajendran S, Zhang Y, et al. Chemical looping combustion of coal in a 5 kW_{th} interconnected fluidized bed reactor using hematite as oxygen carrier. Appl Energy 2015;157:304–13.

[20] Chen L, Bao J, Kong L, Combs M, Nikolic H, Fan Z, et al. Activation of ilmenite as an oxygen carrier for solid-fueled chemical looping combustion. Appl Energy 2017;197:40–51.

[21] Sun Z, Lu D, Ridha F, Hughes R, Filippou D. Enhanced performance of ilmenite modified by CeO_2, ZrO_2, NiO, and Mn_2O_3 as oxygen carriers in chemical looping combustion. Appl Energy 2017;195:303–15.

[22] Wen Y, Li Z, Xu L, Cai N. Experimental study of natural Cu ore particles as oxygen carriers in chemical looping with oxygen uncoupling (CLOU). Energ Fuel 2012;26:3919–27.

[23] Zhao H, Wang K, Fang Y, Ma J, Mei D, Zheng C. Characterization of natural copper ore as oxygen carrier in chemical-looping with oxygen uncoupling of anthracite. Int J Greenh Gas Con 2014;22:154–64.

[24] Wang K, Zhao H, Tian X, Fang Y, Ma J, Zheng C. Chemical-looping with oxygen uncoupling of different coals using copper ore as an oxygen carrier. Energ Fuel 2015;29:6625–35.

[25] Wang K, Tian X, Zhao H. Sulfur behavior in chemical-looping combustion using a copper ore oxygen carrier. Appl Energy 2016;166:84–95.

[26] Tian X, Zhao H, Wang K, Ma J, Zheng C. Performance of cement decorated copper ore as oxygen carrier in chemical-looping with oxygen uncoupling. Int J Greenh Gas Con 2015;41:210–8.

[27] Tian X, Wang K, Zhao H, Su M. Chemical looping with oxygen uncoupling of high-sulfur coal using copper ore as oxygen carrier. Proc Combust Inst 2017;36:3381–8.

[28] Arjmand M, Leion H, Mattisson T, Lyngfelt A. Investigation of different manganese ores as oxygen carriers in chemical-looping combustion (CLC) for solid fuels. Appl Energy 2014;113:1883–94.

[29] Mei D, Mendiara T, Abad A, de Diego LF, Garcia-Labiano F, Gayan P, et al. Evaluation of manganese minerals for chemical looping combustion. Energ Fuel 2015;29:6605–15.

[30] Xu L, Sun H, Li Z, Cai N. Experimental study of copper modified manganese ores as oxygen carriers in a dual fluidized bed reactor. Appl Energy 2016;162:940–7.

[31] Haider S, Azimi G, Duan L, Anthony E, Patchigolla K, Oakey J, et al. Enhancing properties of iron and manganese ores as oxygen carriers for chemical looping processes by dry impregnation. Appl Energy 2016;163:41–50.

[32] Bao J, Li Z, Cai N. Promoting the reduction reactivity of ilmenite by introducing foreign ions in chemical looping combustion. Ind Eng Chem Res 2013;52:6119–28.

[33] Wang S, Wang G, Jiang F, Luo M, Li H. Chemical looping combustion of coke oven gas by using Fe_2O_3/CuO with $MgAl_2O_4$ as oxygen carrier. Energy Environ Sci 2010;3:1353–60.

[34] Siriwardane RV, Ksepko E, Tian H, Poston J, Simonyi T, Sciazko M. Interaction of iron-copper mixed metal oxide oxygen carriers with simulated synthesis gas derived from steam gasification of coal. Appl Energy 2013;107:111–23.

[35] Wang B, Yan R, Zhao H, Zheng Y, Liu Z, Zheng C. Investigation of chemical looping combustion of coal with $CuFe_2O_4$ oxygen carrier. Energ Fuel 2011;25:3344–54.

[36] Siriwardane R, Tian H, Simonyi T, Poston J. Synergetic effects of mixed copper-iron oxides oxygen carriers in chemical looping combustion. Fuel 2013;108:319–33.

[37] He F, Galinsky N, Li F. Chemical looping gasification of solid fuels using bimetallic oxygen carrier particles–feasibility assessment and process simulations. Int J Hydrogen Energ 2013;38:7839–54.

[38] Yang W, Zhao H, Wang K, Zheng C. Synergistic effects of mixtures of iron ores and copper ores as oxygen carriers in chemical-looping combustion. Proc Combust Inst 2015;35:2811–8.

[39] Song T, Shen L, Guo W, Chen D, Xiao J. Enhanced reaction performance with hematite/$Ca_2Al_2SiO_7$ oxygen carrier in chemical looping combustion of coal. Ind Eng Chem Res 2013;52:9573–85.

[40] Xu L, Wang J, Li Z, Cai N. Experimental study of cement-supported CuO oxygen carriers in chemical looping with oxygen uncoupling (CLOU). Energ Fuel 2013;27:1522–30.

[41] Mattisson T, Johansson M, Lyngfelt A. Multicycle reduction and oxidation of different types of iron oxide particles application to chemical-looping combustion. Energ Fuel 2004;18:628–37.

[42] Johansson E, Mattisson T, Lyngfelt A, Thunman H. A 300 W laboratory reactor system for chemical-looping combustion with particle circulation. Fuel 2006;85:1428–38.

[43] Mattisson T, Lyngfelt A, Leion H. Chemical-looping with oxygen uncoupling for combustion of solid fuels. Int J Greenh Gas Con 2009;3:11–9.

[44] Abad A, Adánez J, García-Labiano F, Luis F, Gayán P, Celaya J. Mapping of the range of operational conditions for Cu-, Fe-, and Ni-based oxygen carriers in chemical-looping combustion. Chem Eng Sci 2007;62:533–49.

[45] Siriwardane R, Riley J, Tian H, Richards G. Chemical looping coal gasification with calcium ferrite and barium ferrite via solid–solid reactions. Appl Energy 2016;165:952–66.

[46] Shulman A, Cleverstam E, Mattisson T, Lyngfelt A. Manganese/iron, manganese/nickel, and manganese/silicon oxides used in chemical-looping with oxygen uncoupling (CLOU) for combustion of methane. Energ Fuel 2009;23:5269–75.